Development of a flashlamp-pumped Cr:LiSAF laser operating at 30 Hz

Ricardo Elgul Samad, Gesse Eduardo Calvo Nogueira, Sonia Licia Baldochi, and Nilson Dias Vieira, Jr.

Cr^{3+}:$LiSrAlF_6$ crystals are an interesting laser medium because of their spectroscopic characteristics: They present a broad emission band in the near infrared and can be pumped either by a flashlamp or by diodes. Up to now, their limitation has been mostly due to their poor thermal properties that limit the laser performance either in the repetition rate in a pulsed system or output power in cw systems. We have designed and constructed a flashlamp-pumped laser using a standard rod pumping cavity that avoids most of the heat generated in the pumping process and allows operation at a fairly high repetition rate of 30 Hz with a high average power of 20 W in a conservative operation mode. © 2006 Optical Society of America

OCIS codes: 140.4780, 140.6810, 140.5680, 140.4480, 140.3410.

1. Introduction

Single crystals of Cr:LiSAF (Cr^{3+}:$LiSrAlF_6$) show attractive optical spectroscopic properties[1] for a potential laser medium, such as a long lifetime of the upper laser level (~67 μs) at room temperature,[2] three broad absorption bands,[2] and a wide emission band ranging from 650 to 1050 nm. Laser action was demonstrated under several pumping schemes,[2–5] particularly in cw[6] and pulsed regimes. Pulse durations ranging from hundreds of microseconds under free-running pulsed excitation down to nanoseconds in *Q*-switching and a few femtoseconds in a mode-locking regime[7] were achieved.

Flashlamp-pumped Cr:LiSAF tunable lasers[3,8–10] have been developed that reach pulse energies up to 8.8 J, and flashlamp-pumped ultrashort-pulse amplifiers[10–13] reach peak powers up to 8.5 TW. Because of the poor thermal properties of the LiSAF host,[14] the operation repetition rate of these lasers and amplifiers were always confined either to the single-pulse regime or up to 12 Hz.[8] The low thermal conductivity leads to crystal cracking because of thermally induced stress, and in the case of a gain medium in the shape of a rod, fracture was observed at 18 Hz.[15] In addition to the thermally induced stress that leads to fracture, the lifetime of the Cr:LiSAF laser transition is strongly temperature dependent, dropping from ~67 μs at room temperature to half this value at 69 °C due to thermal quenching.[16] Under flashlamp pumping, the low LiSAF thermal conductivity prevents heat extraction from the laser medium. If the crystal temperature rises above ~25 °C, the nonradioactive decay generates more heat, that in turn increases the nonradioactive decay rate, rapidly increasing the crystal temperature. This is a catastrophic process that reduces the energy storage capacity of the crystal and can lead to fracture.

To avoid thermal quenching and crystal fracture due to accumulated heat, flashlamp-pumped Cr:LiSAF oscillators have been kept operating at low repetition rates. Shimada *et al.*[8] reported the highest repetition rate and power on a Cr:LiSAF laser to be 4.5 W at 12 Hz, and Perry *et al.*[17] reported the highest amplifier repetition rate to be 10 Hz. Alternatively, a slab geometry laser[9] scheme requires small thickness of the gain medium, allowing for better heat extraction and therefore lower stress in the gain medium, and in this case the laser achieved pulse energies as high as 8.8 J but at a 5 Hz repetition rate.

Aiming to raise the repetition rate of flashlamp-pumped Cr:LiSAF lasers and still keep its gain and power, we propose a different approach that minimizes the crystal thermal load and temperature

The authors are with the Instituto de Pesquisas Energética e Nucleares, Commissão Nacional de Energia Nuclear São Paulo, Centro de Lasers e Aplicações, Avenida Professor Lineu Prestes 2242, São Paulo 05508-000, Brazil. R. E. Samad's e-mail address is resamad@gmail.com.

Received 28 October 2005; accepted 26 November 2005; posted 7 December 2005 (Doc. ID 65580).

0003-6935/06/143356-05$15.00/0

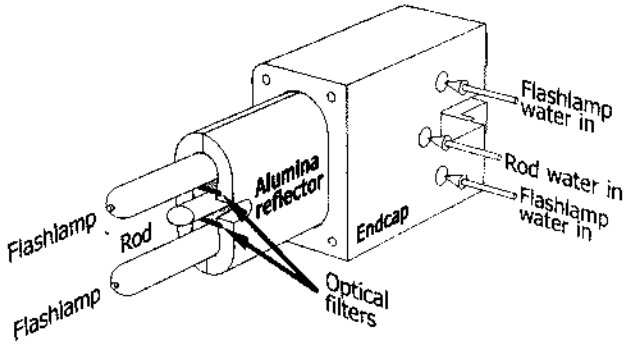

Fig. 1. Scheme of the pumping cavity without an endcap. The different cooling water entrances for refrigerating the crystal and flashlamps are indicated; the optical filters, located between each flashlamp and the crystal, divide the pumping cavity into three independent cooling chambers.

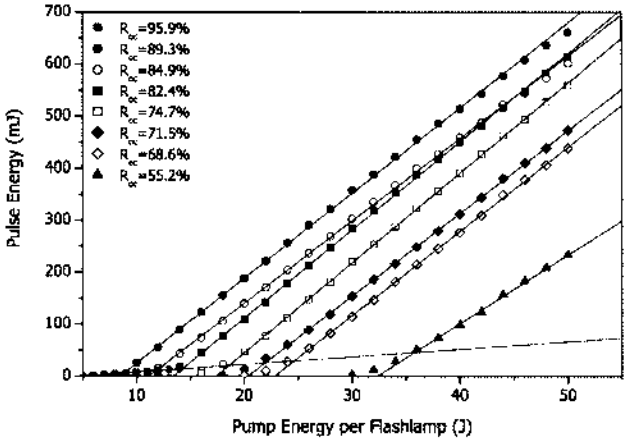

Fig. 2. Cr:LiSAF laser slope efficiencies for various output coupler reflectivities (R_{OC}) along with linear fitted functions for each output coupler, as a function of the pump energy per flashlamp. For each R_{OC} data set, the two or three lower energy points were disregarded in the fitting because of the unstable laser oscillation near the threshold. Error bars were taken into account in each fitting but are not shown in the graph because they are smaller than the symbols used in the plot.

gradient by decreasing the heat reaching the gain medium and being generated inside it. This scheme allows laser operation at repetition rates as high as 30 Hz, with an average power of 20 W.

2. Pumping Cavity Conception and Laser Design

We developed a flashlamp-pumped pumping cavity, aiming to minimize the rod thermal load and to increase the laser repetition rate. The rod has a 1.5 mol.% Cr doping, 101.6 mm of length, and 6.35 mm of diameter, with Brewster-angled faces. Small diameters allow the extraction of heat more efficiently from the bulk of the rod, decreasing the temperature gradient that leads to rod fracture. The cavity has two 4 in. arc length (1 in. = 2.54 cm), 7 mm bore, 450 Torr xenon flashlamps, each one independently fed by a power source capable of delivering up to 50 J in ~67 μs pulses. The power sources were triggered and synchronized by a Stanford Research Systems DG535 delay generator. The pulse width was chosen to match the laser transition lifetime, consequently decreasing heat generation by pump energy that is lost to spontaneous emission. The cavity is a closed coupled one, with an alumina diffuse reflector, and is cooled by de-ionized water at 11 °C in a turbulent flow regime. The humidity in the laboratory is kept under 40%, lowering the dew point, avoiding water condensation on the rod surfaces.

The temperature of the laser medium inside a pumping cavity is determined by how much energy is absorbed by the medium, the amount of that energy that is not converted into light emission (spontaneous or stimulated), and how this excess energy is extracted. The main heat source for the Cr:LiSAF crystal is the Stokes shift from the three absorption bands centered at 290, 450, and 650 nm to the emission band at 850 nm. For a photon absorbed at the center of the 290 nm band resulting in an emitted photon at 850 nm, ~65% of its energy is converted into heat due to the Stokes shift. For photons absorbed at the center of the 430 and 650 nm bands, these fractions are 50% and 24%, respectively. With the purpose of minimizing the heat in the rod, optical filters were inserted into the pumping cavity between the rod and each one of the flashlamps, absorbing all light below 600 nm and above 700 nm. In this way, only the 650 nm band is excited, decreasing the Stokes-shift-generated heat to only ~25% of the absorbed power. In addition, the filters also block the infrared heat component radiating from the flashlamps. The pumping cavity was designed in a way that the optical filters divide it in three compartments, isolating the rod from the flashlamps, allowing independent coolant flow around each component. The cooling water flows around the rod and then refrigerates the flashlamps. Thus heat transfer from the flashlamps to the rod by the cooling water is avoided. In Fig. 1 a scheme of the pumping cavity is shown.

The optical resonator was built using a 1 m curvature radius concave high-reflector mirror located 21 cm away from one rod end and a plane output coupler located 12 cm from the other end of the rod, resulting in a stability product[18] $g_1g_2 = 0.57$ for an empty resonator. Plane output couplers with reflections ranging from 55% to 96% at 850 nm were used to characterize the laser performance.

3. Results

The laser output pulse energy as a function of one of the flashlamps input energy, for eight different output coupler reflectivities (R_{OC}), is shown in Fig. 2. The data for the highest reflectivity (R_{OC} = 95.9%) output coupler are limited to energies under 14 J/flashlamp because the mirror was damaged at that pump energy due to absorption losses. In Table 1 we present the total (two flashlamps) pump energy threshold for laser action for each output coupler and the corresponding slope efficiencies. The maximum total measured efficiency is 0.65% for R_{OC} = 89.3% and 100 J pumping energy. In Fig. 3

Table 1. Values Obtained from the Fitted Functions Shown in Fig. 2 for Each Output Coupler

R_{OC} (%)	$\ln(R_{OC})$	E_{th} (J)	Slope Efficiency (%)	$g_t l$
95.9 ± 1.0	0.042 ± 0.010	8.68 ± 0.28	0.072 ± 0.001	0.045 ± 0.006
89.3 ± 0.4	0.113 ± 0.004	16.96 ± 0.24	0.818 ± 0.004	0.081 ± 0.005
84.9 ± 0.6	0.164 ± 0.007	22.28 ± 0.22	0.792 ± 0.004	0.106 ± 0.006
82.4 ± 0.5	0.193 ± 0.006	26.86 ± 0.22	0.848 ± 0.003	0.121 ± 0.005
74.7 ± 0.6	0.292 ± 0.008	34.80 ± 0.24	0.865 ± 0.003	0.170 ± 0.006
71.5 ± 0.5	0.335 ± 0.007	40.68 ± 0.34	0.799 ± 0.004	0.192 ± 0.006
68.6 ± 0.5	0.377 ± 0.007	45.64 ± 0.46	0.810 ± 0.005	0.212 ± 0.006
55.2 ± 0.5	0.594 ± 0.009	64.7 ± 2.0	0.66 ± 0.01	0.321 ± 0.006

the spectrum of the laser operating with the R_{OC} = 89.3% output coupler, measured by a Spiricon ultrafast laser spectrometer, is shown and the data are fitted by a Gaussian profile. The emission is centered at 851 nm and has a bandwidth (FWHM) of 6.4 nm. The small spikes observed at 847.5, 849, 851, and 858 nm are due to spectrometer imperfections. Figure 4 shows the temporal evolution of the laser pulses for R_{OC} = 89.3% under 100 J pumping. The measured laser output pulse width (FWHM) is approximately 65 μs and does not change significantly along the pumping energy range.

From the data in the second and third columns of Table 1, the resonator losses were determined through a Findlay–Clay analysis.[19] This analysis consists of fitting a line to the data of $-\ln(R_{OC})$ as a function of the lasing threshold pump energy, and the resonator losses are given by the point where the line crosses the y axis. The data fitted by the line are shown in Fig. 5, resulting in total resonator losses L with a value L = (4.8 ± 0.9)%. It is then possible to calculate the threshold gain, given by[18]

$$g_t l = \frac{1}{2}\,[L - \ln(R_{OC})], \tag{1}$$

where g_t is the threshold small-signal gain and l is the rod length. From Eq. (1) the threshold gain can be determined for each output coupler, and the values are shown in the fifth column of Table 1.

Figure 6 shows the pulse energy dependence on the pump repetition rate. It can be seen that for a 60 J pumping level, the pulse energy is almost constant, varying ~3% around its average value. For higher pump energies, a decrease of the pulse energy with increasing repetition rate is observed. At 100 J and 30 Hz, this pulse energy drop is 8% of its value at 1 Hz. The maximum measured pulse energy at 30 Hz is (660.4 ± 9.4) mJ, resulting in pulses with peak power of over 10 kW and an average power of 19.8 W.

To investigate whether this energy dropping, at higher repetition rates, is due to the lifetime shortening as a consequence of rod heating and thermal quenching, the temporal shapes of the flashlamp pulse and of the spontaneous emission were measured with fast detectors and an averaging oscilloscope (LeCroy WaveRunner 6051) for various repetition rates at the higher pump energy (100 J). An empirical function was fitted to the flashlamp's emission temporal shape, and this fitted function was used as the pumping term $I_p(t)$ to numerically

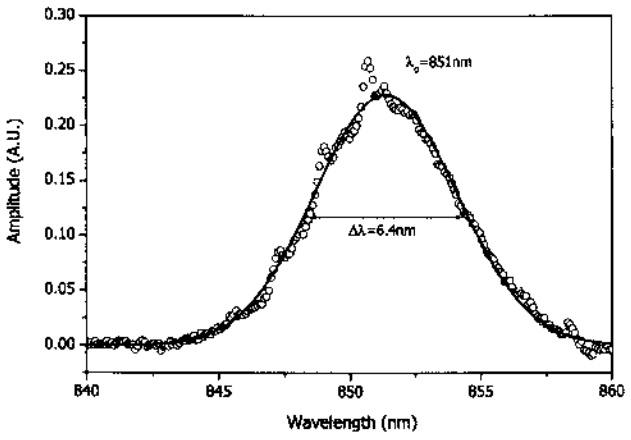

Fig. 3. Cr:LiSAF laser spectrum with R_{OC} = 89.3% output coupler measured at 80 J energy and 10 Hz repetition rate. The spikes observed at 847.5, 849, 851, and 858 nm are due to spectrometer imperfections.

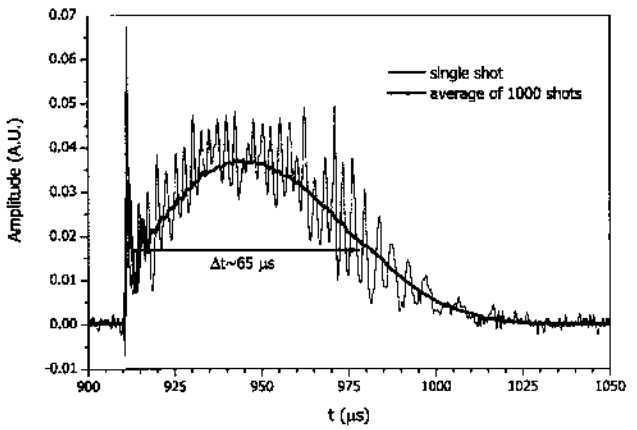

Fig. 4. Temporal evolution of the laser pulses at 100 J for the R_{OC} 89.3% output coupler. The thin curve is a single shot and the thick curve is the average of 1000 shots. The width (FWHM) is indicated for the average curve. The time axis starts at 900 μs due to the relative delay between the trigger and the detector signals.

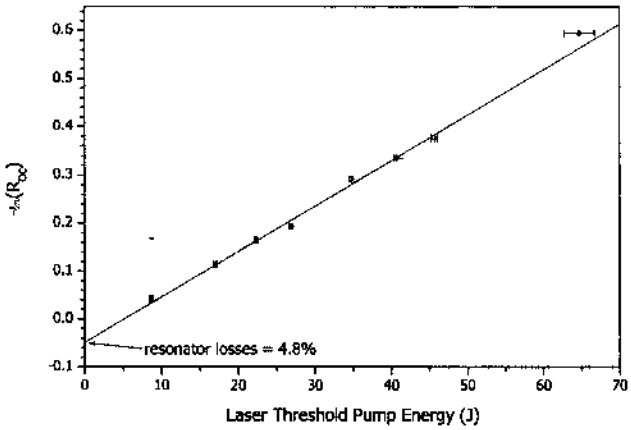

Fig. 5. Findlay–Clay analysis of the laser. The fitted line crosses the y axis at -0.048, providing the resonator losses.

solve the population rate equation for the Cr:LiSAF system:

$$\frac{dN_2}{dt} = N_0 I_p(t) - \frac{N_2}{\tau}, \tag{2}$$

where N_0 and N_2 are the Cr^{3-} ground- and excited-state populations, respectively, and the spontaneous emission follows the excited-state population $N_2(t)$. The lifetime of the excited state τ was considered as an adjustable parameter and was tuned to obtain the best agreement between the acquired data for the spontaneous emission and the $N_2(t)$ curve resulting from the numerical integration of Eq. (2). This was done for 100 J pumping and repetition rates ranging from 2 to 30 Hz. For all repetition rates, the best agreement between the experimental and the numerical Cr:LiSAF spontaneous emission curves always occurs for $\tau = 64$ μs, although the flashlamp pulse duration increases almost 5% from 4 to 30 Hz. In Fig. 7 the measured flashlamp's emission and rod spontaneous emission temporal profiles are presented together with the flashlamp temporal fit and

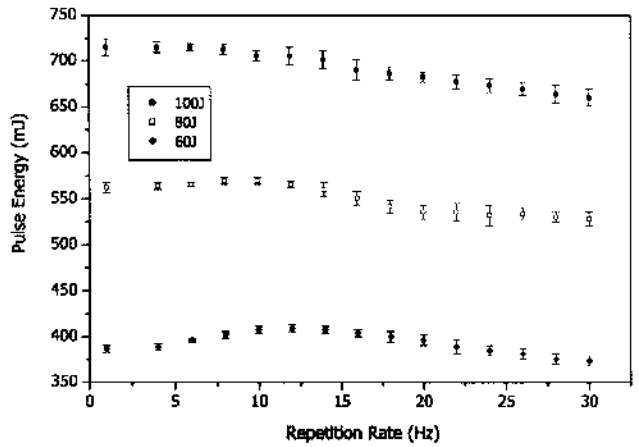

Fig. 6. Dependence of the pulse energy on the pump repetition rate for different pumping energies. The output coupler reflectivity is R_{OC} = 89.3%.

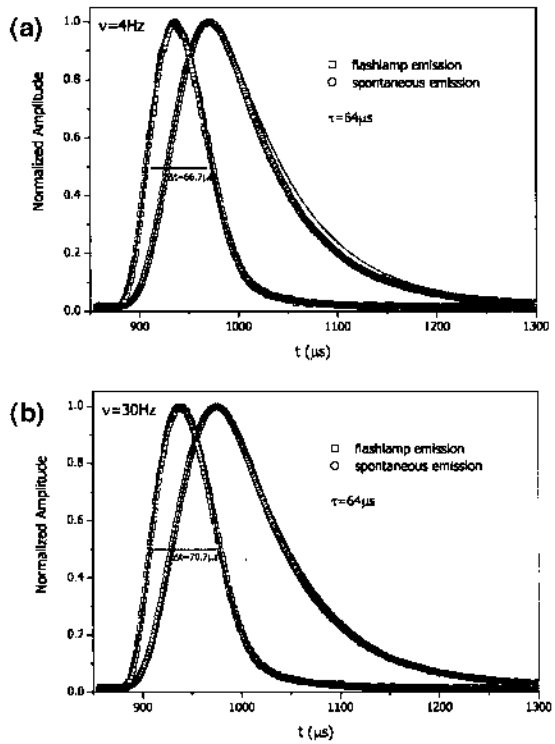

Fig. 7. (Color online) Experimental measured flashlamp emission at 100 J (open squares) and Cr:LiSAF spontaneous emission (open circles), with the empirical function fitted to the flashlamps emission and the numerical solution of the Cr:LiSAF rate equation for τ = 64 μs (solid curves), normalized to (peak amplitude) = 1. In the curves for (a) 4 Hz and (b) 30 Hz, the flashlamp pulse duration (FWHM) is indicated. The time axis starts at 850 μs due to the relative delay between the trigger and the detector signals.

the emission numeric solution for 4 and 30 Hz repetition rates. The criterion for checking the agreement between the data and the numerical solution was the emission peak position. The spontaneous emission decay was not chosen because the fitted function to the flashlamp's emission drops slower than the measured data and consequently causes a slower spontaneous emission decay. The fact that the same lifetime (64 μs) provided the best agreement for all repetition rates from 2 to 30 Hz indicates that there is no quenching of the luminescence due to the increased thermal load in the crystal as the repetition rate grows. The energy drop shown in Fig. 6 is probably due to slight changes in the flashlamp and power source behavior and efficiency as the repetition rate increases. Although the absolute value obtained for the Cr:LiSAF lifetime differs from the accepted one[2] of (67 ± 5) μs, it is within its precision measurement. Nevertheless, the value agrees with the one measured[16] at 77 K that is predicted to be the same at room temperature.

4. Conclusions

We have developed a flashlamp-pumped Cr:LiSAF resonator with a reduced thermal load in the crystal rod, so the laser repetition rate could be increased. The final repetition rate is over the reported values at

which the rod is damaged. The laser performance was characterized providing fundamental parameters as resonator losses and threshold gain. Although the efficiency was reduced by the insertion of filters that prevented the pumping of the higher-energy absorption bands, a threshold gain over 0.3 was measured and the laser could be operated at 30 Hz with an average power of 20 W and a peak power in excess of 10 kW. No noticeable decrease in the lifetime of the laser transition was observed in the range of repetition rates used, implying that our design could avoid significant laser rod temperature rise at high repetition rates. This indicates that the laser can be operated at even higher repetition rates and higher powers. Also, the developed pumping cavity can be used as an amplifying medium for ultrashort-pulse systems, being operated at repetition rates higher than the ones already reported.

The authors thank Wagner de Rossi for helpful discussions for the design of the pumping cavity and the Fundação de Amparo à Pesquisa do Estado de São Paulo for financial support under the grant 00/15135-9.

References

1. S. A. Payne, L. L. Chase, and G. D. Wilke, "Optical spectroscopy of the new laser materials, $LiSrAlF_6$-Cr^{3+} and $LiCaAlF_6$-Cr^{3+}," J. Lumin. **44,** 167–176 (1989).
2. S. A. Payne, L. L. Chase, L. K. Smith, W. L. Kway, and H. W. Newkirk, "Laser performance of $LiSrAlF_6$:Cr^{3+}," J. Appl. Phys. **66,** 1051–1065 (1989).
3. M. Stalder, B. H. T. Chai, and M. Bass, "Flashlamp pumped Cr:$LiSrAlF_6$ laser," Appl. Phys. Lett. **58,** 216–218 (1991).
4. R. Scheps, J. F. Myers, H. B. Serreze, A. Rosenberg, R. C. Morris, and M. Long, "Diode-pumped Cr:$LiSrAlF_6$ laser," Opt. Lett. **16,** 820–822 (1991).
5. B. Agate, A. J. Kemp, C. T. A. Brown, and W. Sibbett, "Efficient, high repetition rate femtosecond blue source using a compact Cr:LiSAF laser," Opt. Express **10,** 824–831 (2002).
6. M. Ihara, M. Tsunekane, N. Taguchi, and H. Inaba, "Widely tunable, single-longitudinal-mode, diode pumped CW Cr:LiSAF laser," Electron Lett. **31,** 888–889 (1995).
7. S. Uemura and K. Torizuka, "Generation of 12-fs pulses from a diode-pumped Kerr-lens mode-locked Cr:LiSAF laser," Opt. Lett. **24,** 780–782 (1999).
8. T. Shimada, J. W. Early, and N. J. Cockroft, "Repetitively pulsed Cr:LiSAF for LIDAR applications," in *Advanced Solid-State Lasers*, Vol. 20 of OSA Trends in Optics and Photonics Series (Optical Society of America, 1994), pp. 188–191.
9. D. E. Klimek and A. Mandl, "Power scaling of a flashlamp-pumped Cr:LiSAF thin-slab zig-zag laser," IEEE J. Quantum Electron. **38,** 1607–1613 (2002).
10. H. Takada, K. Miyazaki, and K. Torizuka, "Flashlamp-pumped Cr:LiSAF laser amplifier," IEEE J. Quantum Electron. **33,** 2282–2285 (1997).
11. W. E. White, J. R. Hunter, L. Van Woerkom, T. Ditmire, and M. D. Perry, "120-fs terawatt $Ti:Al_2O_3$/Cr:$LiSrAlF_6$ laser system," Opt. Lett. **17,** 1067–1069 (1992).
12. P. Beaud, M. Richardson, E. J. Miesak, and B. H. T. Chai, "8-TW 90-fs Cr:LiSAF laser," Opt. Lett. **18,** 1550–1552 (1993).
13. T. Ditmire, H. Nguyen, and M. D. Perry, "Amplification of femtosecond pulses to 1 J in Cr:$LiSrAlF_6$," Opt. Lett. **20,** 1142–1144 (1995).
14. S. A. Payne, L. K. Smith, R. J. Beach, B. H. T. Chai, J. H. Tassano, L. D. DeLoach, W. L. Kway, R. W. Solarz, and W. F. Krupke, "Properties of Cr:$LiSrAlF_6$ crystals for laser operation," Appl. Opt. **33,** 5526–5536 (1994).
15. F. Hanson, C. Bendall, and P. Poirier, "Gain measurements and average power capabilities of Cr^{3+}:$LiSrAlF_6$," Opt. Lett. **18,** 1423–1425 (1993).
16. M. Stalder, M. Bass, and B. H. T. Chai, "Thermal quenching of fluorescence in chromium-doped fluoride laser crystals," J. Opt. Soc. Am. B **9,** 2271–2273 (1992).
17. M. D. Perry, D. Strickland, T. Ditmire, and F. G. Patterson, "Cr:$LiSrAlF_6$ regenerative amplifier," Opt. Lett. **17,** 604–606 (1992).
18. W. Koechner, *Solid-State Laser Engineering* (Springer-Verlag, 1999).
19. D. Findlay and R. A. Clay, "Measurement of internal losses in 4-level lasers," Phys. Lett. **20,** 277–278 (1966).